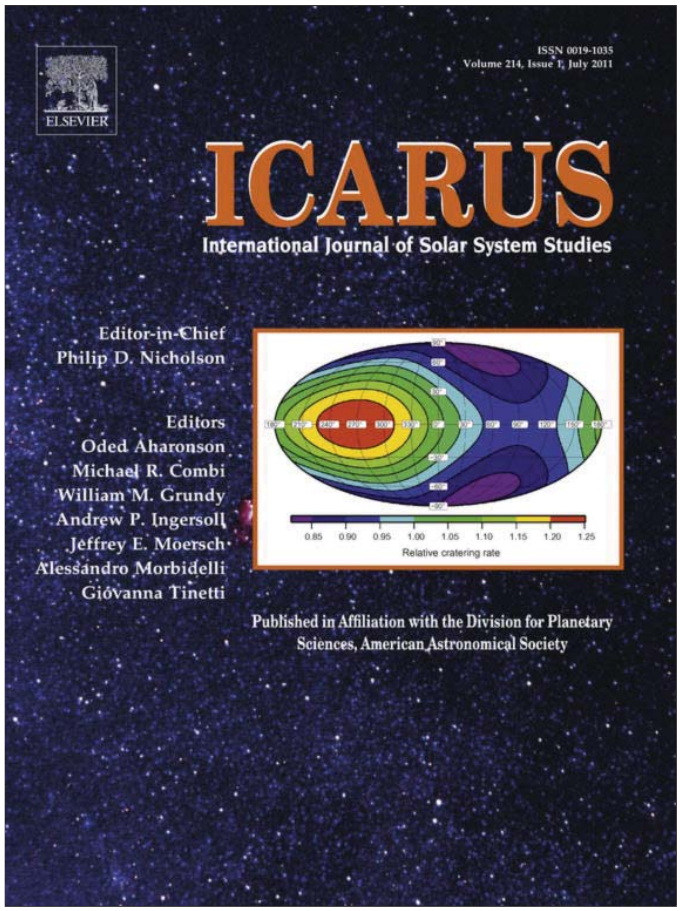

Icarus 214 (2011) 240–245

Contents lists available at ScienceDirect

Icarus

journal homepage: www.elsevier.com/locate/icarus

# Assessing spectral evidence of aqueous activity in two putative martian paleolakes

Ted L. Roush [a,*], Giuseppe A. Marzo [a,b,1], Sergio Fonti [c], Vincenzo Orofino [c], Armando Blanco [c], Christoph Gross [d], Lorenz Wendt [d]

[a] NASA Ames Research Center, MS 245-3 Moffett Field, CA 94035-0001, United States
[b] Bay Area Environmental Research Institute, 560 Third St. West, Sonoma, CA 95476, United States
[c] Dipartimento di Fisica, Università del Salento, Via Arnesano, 73100 Lecce, Italy
[d] Freie Universität Berlin, Institute of Geological Sciences, Planetary Sciences and Remote Sensing, Malteserstr. 74-100 12449 Berlin, Germany

ARTICLE INFO

*Article history:*
Received 26 January 2011
Revised 20 April 2011
Accepted 21 April 2011
Available online 29 April 2011

*Keywords:*
Mars, Surface
Infrared observations
Spectroscopy
Mineralogy
Astrobiology

ABSTRACT

We evaluate the evidence for the presence of mineral spectral signatures indicative of the past presence of water at two putative paleolakes on Mars using observations by the Mars Reconnaissance Orbiter (MRO) Compact Reconnaissance Image Spectrometer for Mars (CRISM). CRISM spectra of both sites are consistent with laboratory spectra of Mg-rich phyllosilicates. Our analysis represents the first detailed evaluation of these locations. The spatial occurrence and association with topographic features within the craters is distinctly different for the two sites. The occurrence of these minerals supports the conclusion that water was once active in the areas sampled by these craters. The distribution of the phyllosilicates in Luqa does not provide distinctive evidence for the presence of a previous standing body of water and is consistent with either impact emplacement or post-impact alteration. For Cankuzo, the phyllosilicate distribution provides evidence of a layer in the crater wall indicative of aqueous activity, but does not require a paleolake.

Published by Elsevier Inc.

## 1. Introduction

### 1.1. Putative paleolakes on Mars

Putative paleolakes in martian impact craters have been the subject of local and regional studies as valuable targets for exploration (see Cabrol and Grin, 1999, 2005, and references therein). They have been suggested as landing sites for *in situ* and sample-return missions since they should provide information about the dynamics of the sedimentary processes and the climate under which they were formed, and also represent favorable environments for preserving biomarkers.

A basin is a topographic depression created by erosional, volcanic, tectonic, or impact processes. A closed basin has an input channel(s) and no outflow channel(s) (Forsythe and Blackwelder, 1998). Provided climatic and local hydrographic conditions permit (Cabrol and Grin, 1999), water enters the basin and without an outlet, it is lost via evaporation, sublimation, and/or percolation into the subsurface. If a standing lake is formed in a basin, then a greater time period is available for mineral alteration, and concentration of sediments and chemicals would occur as the water disappears. For episodic water flow there is less time for mineral alteration and any sediments or evaporites formed may be comparable to arid or semi-arid terrestrial environments (Cabrol and Grin, 1999 and references therein).

A relatively water-poor environment can result in formation of evaporites (Stockstill et al., 2005, 2007). The exact chemistry of the deposits depends upon the source materials and the Eh and pH conditions occurring during evaporation (Eugster and Hardie, 1978; Crowley, 1993; Crowley and Hook, 1996). Carbonate- and sulfate-bearing species have spectral features in the visible and near-infrared (vnir) (e.g. Gaffey, 1986, 1987; Calvin et al., 1994; Cloutis et al., 2008) that are likely to remain present under current martian atmospheric conditions (Cloutis et al., 2008). Mars orbital vnir spectral data provide evidence for sulfates (Bibring et al., 2006; Murchie et al., 2009 (Wray et al., 2011 and references therein) and carbonates (Ehlmann et al., 2008a; Palomba et al., 2009; Murchie et al., 2009; Michalski and Niles, 2010 and references in all) in some putative paleolakes.

Phyllosilicates are also materials indicative of aqueous alteration of materials. CRISM data has provided evidence for the presence of several types of phyllosilicates at many locations on Mars including numerous crater exposed deposits. The range of chemistry includes Al- to Fe–Mg-rich materials (Mustard et al., 2008; Ehlmann et al., 2008b; Murchie et al., 2009; Dehouck et al., 2010; Milliken and Bish, 2010; Carter et al., 2009, 2010, 2011; Ansan et al., 2011).

* Corresponding author. Fax: +1 650 604 6779.
*E-mail address:* ted.l.roush@nasa.gov (T.L. Roush).
[1] Present address: ENEA, C.R. Casaccia, UTFISST-RADSITO, Via Anguillarese 301, 00123 S. Maria di Galeria, Roma, Italy.

0019-1035/$ - see front matter Published by Elsevier Inc.
doi:10.1016/j.icarus.2011.04.017

Here we investigate CRISM observations of putative paleolakes on Mars to evaluate the evidence for the presence of mineral spectral signatures indicative of the past presence of water at these sites.

### 1.2. Site selection and background

As part of a larger study of putative paleolakes on Mars (Roush et al., 2009) initial analyses identified signatures of phyllosilicates in only Luqa and Cankuzo craters. Here we focus upon more detailed analyses of these craters. Luqa (~17 km diameter, 18.23S, 131.81E) and Cankuzo (~51 km diameter, 19.39S, 52.05E) craters are closed basins and were selected based upon morphologic features suggestive of the ancient presence of standing bodies of water, specifically the presence of an inlet channel(s) and no outlet channel(s) (Orofino et al., 2009). These craters have well-defined edges and do not appear to have undergone major modification by subsequent impacts.

The floor of Cankuzo is mapped as Hesperian, Hplm, representing one of the youngest units of the plateau sequence (Greeley and Guest, 1987). The basin wall and adjacent floor are mapped as Noachian, $Npl_1$, corresponding to widespread cratered material in the southern highlands (Greeley and Guest, 1987). Luqa is mapped entirely as $Npl_1$ by Greeley and Guest (1987).

Cankuzo and Luqa are not discussed in the studies of Bibring et al. (2006), Stockstill et al. (2005, 2007), Tirsch et al. (2011), Carter et al. (2009, 2010, 2011) or Wray et al. (2009), but are in regions where sheet silicates/high-Si glass may be present (Bandfield, 2002).

## 2. Data analysis

CRISM is a mapping spectrometer that from orbit provides ~18–200 m/pixel spatial sampling (Murchie et al., 2007). The highest spatial resolution (FRT observations) has full spectral sampling of 545 wavelengths, but of limited locations on the martian surface. The lower spatial resolution (MSP observations) have only ~70 wavelengths, but more extensive spatial coverage of Mars (Murchie et al., 2007).

The CRISM data are from the Planetary Data System and locations of observations are shown in Fig. 1a and e. The CRISM data were converted to apparent I/F (reflected/incident sunlight), then divided by the cosine of the incidence angle to correct for the

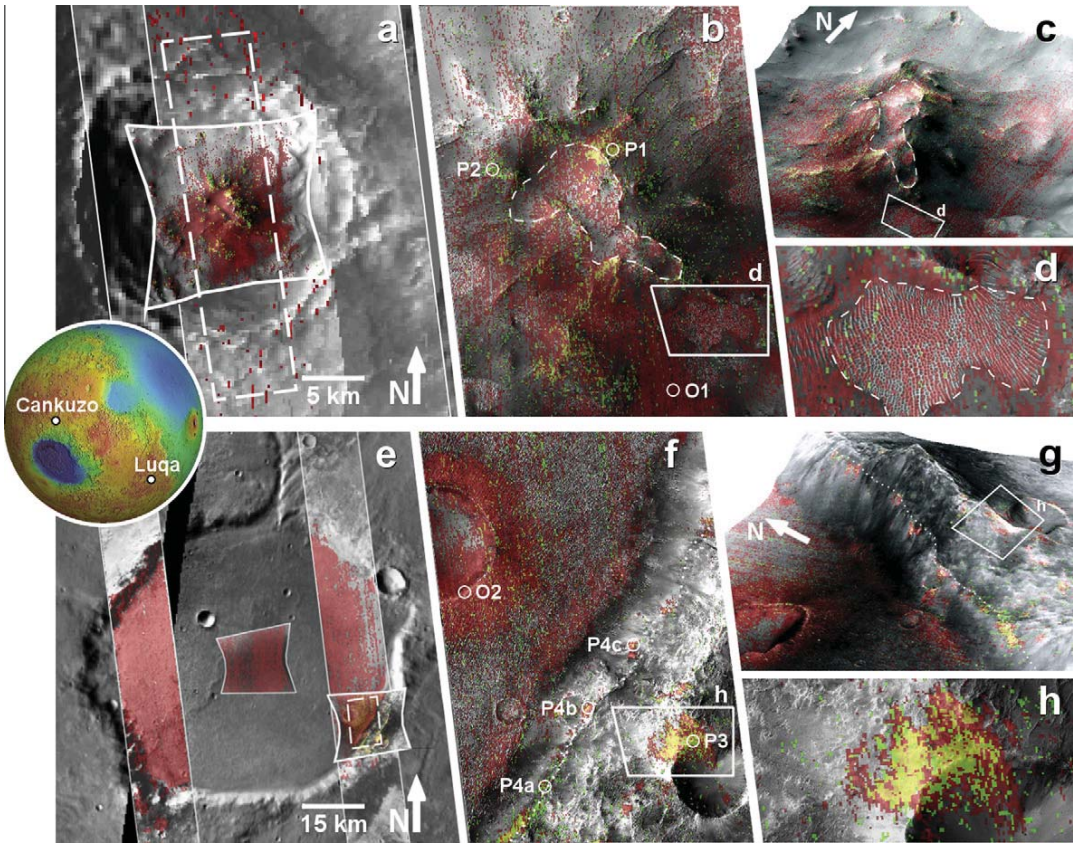


**Fig. 1.** Round inset – locations of Cankuzo and Luqa craters, Mars. (a) MRO observations at Luqa. Thin solid white lines and hourglass shape are boundaries of CRISM MSP and FRT observation, respectively. All values are >0.0 and are red for OLV2 and green for D2300; yellow is where both occur. The dashed line is the boundary of HiRISE observation ESP_013527_1615. (b) Overlay of CRISM and HiRISE data in Luqa, thin dashed line is a morphologic feature shown in panel c, the solid outline is a region shown in panel d, and the circles (P1, P2, and O1) are where spectral data were extracted. (c) Perspective view of CRISM observations of Luqa using MOLA topography, the morphologic region from panel b and region of panel d are shown. (d) Enlargement of dunes in panels b and c, values of OLV2 (red) are more pronounced surrounding the dune field, outside the thin dashed line. (e) Same as panel a, but for Cankuzo with HiRISE observation ESP_012541_1600. (f) CRISM observations at Cankuzo are superimposed upon HiRISE. The dotted white line is a series of out-crops, the solid white outline indicates the close-up shown in panel h, and the open circles (O2, P3, P4a, P4b, and P4c) indicate where CRISM spectra were extracted. (g) CRISM observations of Cankuzo using MOLA-derived topography. The dotted white line is the same as in f and the outline shows the area of panel h. (h) Enlargement of the small crater outside the basin showing the distribution of phyllosilicate-bearing materials. (For interpretation of the references to color in this figure legend, the reader is referred to the web version of this article.)

illumination geometry (Murchie et al., 2007, 2009). The atmospheric contribution was removed using a volcano-scan correction (McGuire et al., 2009). A de-spiking and de-striping algorithm (Parente, 2008) was applied to improve the overall quality of the observations. Additionally, co-registration of the observations allows comparisons with other observational products of the area.

Evaluation of the CRISM data used the spectral parameters of Pelkey et al. (2007). Of particular interest are those associated with hydrated and/or hydroxylated silicates (H), sulfates (S), and carbonates (C). These include: BD1750 (S), BD2100 (S), BD2210 (H), BD2290 (H), D2300 (H), D2400 (S), BDCARB (C), and BD3400 (C). Each parameter map was visually evaluated using one, or more, threshold value(s) and when a spatially coherent pattern was identified, confirmation of the identification involved extraction of individual spectra. Once confirmed, the spatial distributions of the materials were evaluated.

High Resolution Imaging Science Experiment (HiRISE, McEwen et al., 2007) observations were coordinated with at least one CRISM FRT observation and the locations are shown in Fig. 1a and 1e. A High Resolution Stereo Camera (HRSC, Neukum et al., 2004) image was used to evaluate the ages of regions at Cankuzo. Two Context Imager (CTX, Malin et al., 2007) images were used to evaluate the ages at Luqa. The modeled age was calculated from the cumulative crater size-frequencies at a reference crater diameter of 1 km, using the established cratering chronology model for Mars (Hartmann and Neukum, 2001; Ivanov, 2001).

## 3. Results

Fig. 1 shows false color versions of the CRISM observations of Luqa (MSP_40A8, MSP_81C2, MSP_74C8, and FRT_112C9) and Cankuzo (MSP_3238, MSP_64DF, FRT_11D18 and FRT_1192C), illustrating spatially coherent patterns of OLINDEX_2 (Salvatore et al., 2010, OLV2 hereafter), related to ferrous iron in minerals including Fe-bearing phyllosilicates (Murchie et al., 2009), and D2300, indicative of phyllosilicates.

Average spectra of Luqa and Cankuzo where a strong OLV2 value was detected (Fig. 2a) can be compared to laboratory reflectance spectra of olivines, low (LCP) and high calcium (HCP) pyroxenes (Fig. 2b). The minima near 1 μm and 2.0–2.5 μm in the CRISM spectra are consistent with HCP. The different minimum position in the 2–2.5 μm region suggests the HCP composition of Luqa is more Mg-rich than in Cankuzo. The width of the minimum near 1 μm suggests a contribution from olivine, although in Luqa the olivine is either less abundant, more Mg-rich, has a different grain size, or is masked by coatings, compared to the olivine in Cankuzo.

Average spectra of locations with high values of D2300 in Luqa and Cankuzo (Fig. 2c) can be compared to laboratory spectra of phyllosilicates (Fig. 2d). The spectra exhibit minima, near 1.92 and 2.32 μm (Luqa) and 2.305 μm (Cankuzo). The first is due to molecular water and the second two to hydroxyl in minerals (e.g. Clark et al., 1990). The minima of Luqa and Cankuzo spectra are consistent with the laboratory spectra of saponite and pyrophyllite-talc, respectively, although a mixture of the minerals shown in Fig. 2d cannot be precluded.

Using crater statistics, Cankuzo has a base age of $3.79^{+0.09}_{-0.27}$ Ga and displays a clear resurfacing at $3.37^{+0.08}_{-0.14}$ Ga of the material filling the basin floor (Fig 3e). The base age determination relies upon two bins, containing 3 craters. Although this is relying upon statistics of small numbers, there is an abrupt transition of bins (Fig. 3e, black points) falling along the older chronology line that shifts to the younger chronology line. Such a transition is consistent with a resurfacing event (Michael and Neukum, 2010). The surface to the northwest of Cankuzo has an age of $3.40^{+0.06}_{-0.10}$ Ga (Fig 3c). The

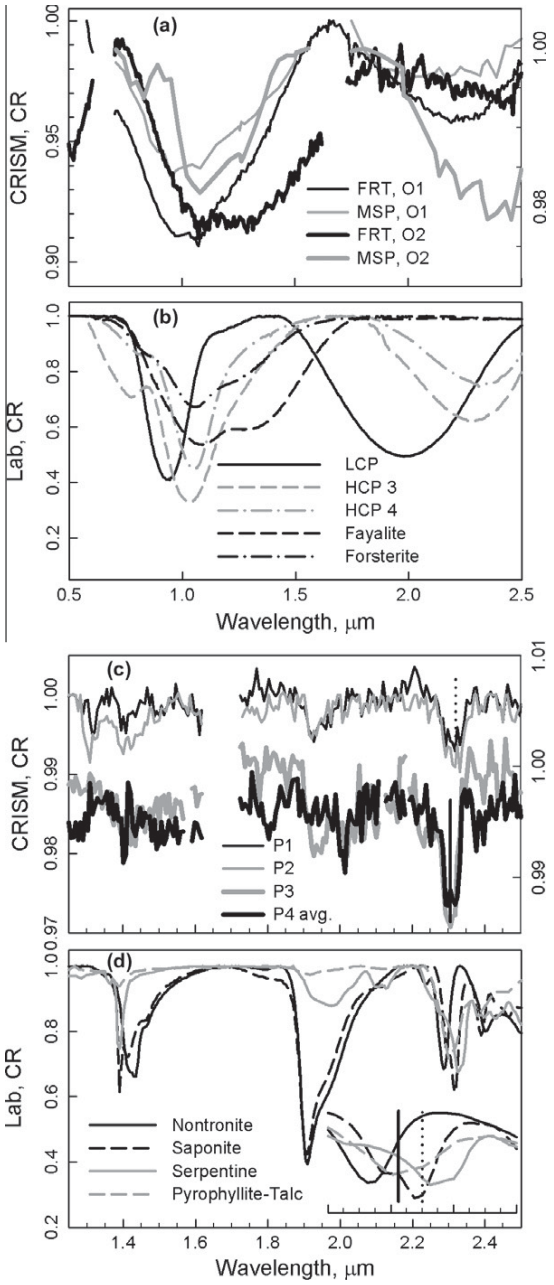


**Fig. 2.** (a) Continuum removed CRISM spectra for Luqa (thin lines, left axis) and Cankuzo (thick lines, right axis). Black and gray lines are for CRISM FRT and MSP observations, respectively. O1 and O2 are spectral averages extracted from the areas in Figs. 1b and d. (b) Continuum removed laboratory spectra of two end-members of olivine (dashed and dash-dot black lines) LCP (solid black line), and HCP (dashed and dash-dot gray lines). (c) Continuum removed CRISM FRT spectra for Luqa (thin lines, left axis) and Cankuzo (thick lines, right axis). P1, and P2, are from areas in Fig. 1b and P3 and P4 are spectral averages from the areas in Fig. 1f. The vertical lines indicate the minimum in the 2.2–2.35 μm region. (d) Continuum removed laboratory spectra of Fe–Mg-bearing phyllosilicates. The inset enlarges the 2.26–2.38 μm region. The vertical lines correspond to the lines in panel c.

nearly contemporaneous age and presence of small and subdued dentritic channels discarging in direction of the Cankuzo observed in the HRSC image both suggest that the eroded surface to the west likely delivered the infilling material seen on Cankuzo's floor between 3.79 and 3.40 Ga. For Luqa, interior was too rough and

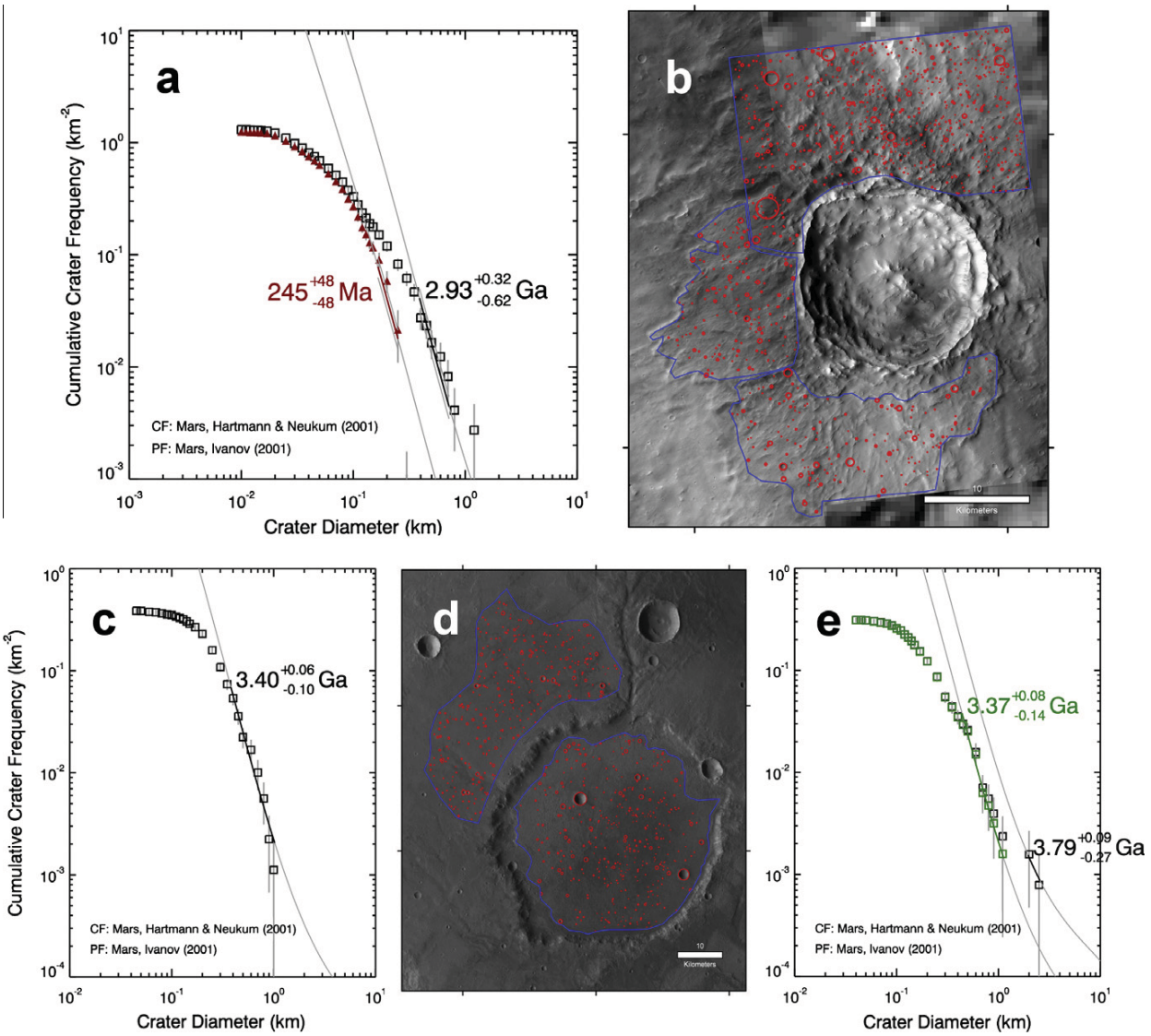


**Fig. 3.** Areas, delineated in blue, used for determination of ages in (b) Luqa (CTX, P13_006196_XN_17S228W and B06_012037_1616_XN_19S228W) and (d) Cankuzo, (HRSC H7225_0010). Red circles indicate craters. (a) Cumulative crater frequencies defining the age for Luqa are determined on the eject blanket (black and red symbols are the base and resurfacing ages, respectively), the plains to the NW of Cankuzo (c) and within Cankuzo (e, black and green symbols are the base and resurfacing ages, respectively). (For interpretation of the references to color in this figure legend, the reader is referred to the web version of this article.)

uneven to obtain a meaningful measurement of craters, as a result we used craters on the ejecta blanket. The cratering statistics yield an age of $2.93^{+0.32}_{-0.62}$ Ga for the ejecta external to Luqa. A resurfacing event, determined using the technique of Michael and Neukum (2010), occurred with an age of 245 ± 48 Ma (Fig. 3a).

## 4. Discussion

We interpret the CRISM spectra to show the presence of secondary minerals (Mg-bearing phyllosilicates) and a primary ferrous-bearing component (HCP and/or olivine) in both craters. The spatial distribution of the secondary minerals is significantly different in the two craters.

At Luqa, the secondary minerals chiefly occur near the central uplift with limited distribution elsewhere (Fig. 1a–c). During the impact, buried, pre-existing sediments can be emplaced in central peaks (e.g. Kenkmann et al., 2005) or dehydrated by transient temperatures (e.g. Marzo et al., 2010; Fairén et al., 2010). However, the areas with high D2300 values are along ridges and at tops of some cone shaped deposits, and are perpendicular to lineaments suggestive of bedding near the central peak. The observed distribution is consistent with alteration due to localized hydrothermal circulation along weak zones induced by the residual heat in the central peak from the impact (e.g. Marzo et al., 2010). Neither the impact exposure nor post-impact hydrothermal alteration scenarios require a standing body of water in Luqa, and selecting between these alternatives likely requires stereo imaging coverage, providing 3-D information.

The OLV2 distribution at Luqa is confined to the southwest crater floor and lower crater wall. CRISM observations (MSP_81C2, not shown here) exhibit a similar OLV2 unit ~60 km to the south but nothing in the intervening area suggesting that aeolian activity is not the emplacement mechanism for OLV2 at Luqa. This

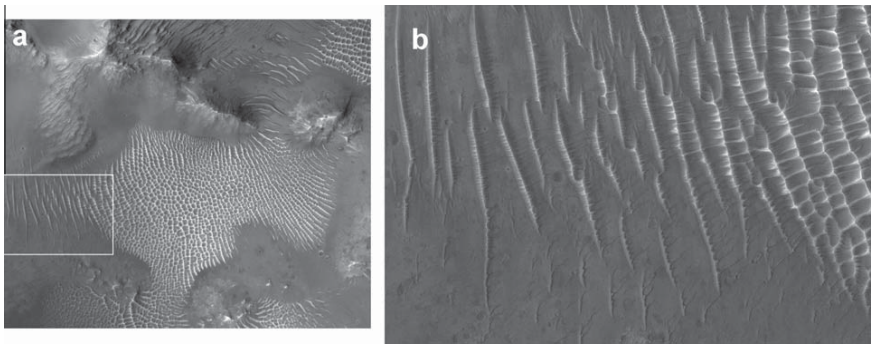


**Fig. 4.** (a) Portion of HiRISE image of dune field in Luqa. Small craters occur in the unit surrounding the dune field but are absent within the dune field. White rectangle indicates region shown in panel b. (b) The dune spacing increases to the west of the dune field shown in panel a. Comparison of this same area to Fig. 1d indicates that the OLV2 index is associated with the underlying and inter-dune regions.

hypothesis is further supported via a dune field within Luqa (Fig. 1d) where the border has a spatially coherent OLV2 pattern. Examination of the HiRISE image (Fig. 4a) shows that the region of the coherent OLV2 pattern has craters down to small sizes, while within the dune field evidence for craters is lacking. Additionally, to the west the dune spacing increases (Fig. 4b) and the contiguous OLV2 pattern becomes more clearly pronounced (compare Figs. 1d and 4b). This suggests the OLV2 unit lies below the dunes. Within the dune field the OLV2 pattern is patchy (Fig. 1d), suggesting the CRISM pixel is sampling both the dunes and underlying materials, yielding a mixed spectral signature, although alternative explanations (e.g. surface photometric behavior or textural differences, or less OLV2-bearing material) cannot be completely ruled out. We speculate the crater impact process exposed the OLV2 unit either by exposing pre-existing material or emplacement of a melt sheet.

The distribution of minerals within Luqa suggests more than one geologic unit and the derived age is inconsistent with the Noachian associated with $Npl_1$ of Greeley and Guest (1987), which suggests mapping of this area should be revisited.

The age of Cankuzo is consistent with the surrounding Noachian $Npl_1$ unit of Greeley and Guest (1987). The OLV2 unit is abundant throughout the floor and the age is consistent with Hplm although its distribution within Cankuzo appears to extend closer to the base of the basin wall compared to the unit of Greeley and Guest (1987). CRISM MSP observations do not reveal a similar unit to the south or north of Cankuzo, suggesting the OLV2 unit is not of aeolian origin. Supporting this interpretation is the close temporal association with the resurfacing event, documented to the northwest (Fig. 3c), initiated by aqueous activity, whose age is consistent with an event that emplaced the material filling the crater floor (Fig. 3e, green points). The OLV2 unit defines a lineament suggesting a layer in the Southeast crater wall (Fig. 1f and g), and another concentration of the OLV2 unit is seen near the small crater outside the southeast rim (Fig. 1f–h). The OLV2 units along the crater wall, and near the small crater, are at best a few pixels in extent (Fig. 2g and f). We investigated $2 \times 2$ or $3 \times 3$ pixel averages from these and some of these average spectra exhibit a $\sim$2.3 μm band suggesting Fe-bearing phyllosilicates, while others did not, suggesting other Fe-bearing materials.

The largest spatial occurrence of the D2300 parameter at Cankuzo is associated with this same small crater (Fig. 1f–h). The absence of a D2300 unit in the surrounding region suggests it is not of aeolian origin. Another D2300 unit occurs as a layer in the southeast basin wall (Fig. 1f and g) that was present when Cankuzo formed. However, existing data do not reveal whether the phyllosilicates were produced via aqueous alteration prior or subsequent to the formation of Cankuzo. In either case, no standing body of water is required as fluids could have circulated within the layer to provide alteration. The small crater excavates to about the same altitude as the lineaments identified in the wall of Cankuzo and spectra from several locations within the wall layer (Fig. 2c) suggests the materials are similar.

## 5. Conclusions

CRISM observations of postulated paleolakes Cankuzo and Luqa craters exhibit spectral features consistent with the activity of water at both sites. The spatial distribution of materials in Luqa suggests either impact emplacement or post-impact alteration. In Cankuzo alteration of a layer may have occurred prior, or subsequent, to the crater formation. In neither case is a standing body of water required to explain the presence of phyllosilicates Nonetheless, the phyllosilicates in both craters indicate they preserve evidence for aqueous activity and as a result may represent locations amenable for preservation of biomarkers.

## Acknowledgments

This research was supported by NASA's Mars Data Analysis Program. CG and LW were supported by the German Science Foundation (DFG) through research grant NE 212/11-1 and the Helmholtz Association through the research alliance *Planetary Evolution and Life*. Initial reviews by Jeffrey Moore and Nathalie Cabrol helped improve the original manuscript. We also thank two anonymous reviewers for their comments.

## References

Ansan, V., Loizeau, D., Mangold, N., Le Mouélic, S., Carter, J., Poulet, F., Dromart, G., et al., 2011. Stratigraphy, mineralogy, and origin of layered deposits inside Terby crater, Mars. Icarus 211, 273–304.

Bandfield, J.L., 2002. Global mineral distributions on Mars. J. Geophys. Res. 107, E6. doi:10.1029/2001JE001510.

Bibring, J.-P., Langevine, Y., Mustard, J.F., Poulet, F., Arvidson, R., Gendrin, A., Gondett, B., Mangold, N., Pinet, P., Forget, F., the OMEGA team, 2006. Global mineralogical and aqueous Mars history derived from OMEGA/Mars express data. Science 312, 400–404.

Cabrol, N.A., Grin, E.A., 1999. Distribution, classification, and ages of martian impact crater lakes. Icarus 142, 160–172.

Cabrol, N.A., Grin, E.A., 2005. Ancient and recent lakes on Mars. In: Tokano, Tetsuya (Ed.), Water and Life on Mars. Springer-Verlag, Berlin, Germany, pp. 235–259.

Calvin, W.M., King, T.V.V., Clark, R.N., 1994. Hydrous carbonates on Mars? Evidence from Mariner 6/7 infrared spectrometer and ground-based telescopic spectra. J. Geophys. Res. 99, 14659–14675.

Carter, J., Poulet, F., Bibring, J.-P., Murchie, S., Langenvin, Y., Mustard, J.F., Gondet, B., 2009. Phyllosilicates and other hydrated minerals on Mars: 2. Detailed analysis. Lunar Planet. Sci. XL, 40 (abstract #2058).

Carter, J., Poulet, F., Bibring, J.-P., Murchie, S.L., 2010. Detection of hydrated silicates in crustal outcrops in the northern plains of Mars. Science 328, 1682–1686.
Carter, J., Poulet, F., Ody, A., Bibring, J.-P., Murchie, S., 2011. Global Distribution, Composition and Setting of Hydrous Minerals on Mars: A Reappraisal. Lunar Planet. Sci. Conf. 42. Lunar and Planetary Institute, Houston, Texas (abstract 2593).
Clark, R.N., King, T.V.V., Klejwa, M., Swayze, G.A., Vergo, N., 1990. High spectral resolution reflectance spectroscopy of minerals. J. Geophys. Res. 95, 12653–12680.
Cloutis, E.A., Craig, M.A., Kruzelecky, R.V., Jamroz, W.R., Scott, A., Hawthorne, F.C., Mertzman, S.A., 2008. Spectral reflectance properties of minerals exposed to simulated Mars surface conditions. Icarus 195, 140–168.
Crowley, J.K., 1993. Mapping playa evaporite minerals AVIRIS data: A first report from Death Valley, California. Remote Sens. Environ. 44, 337–356.
Crowley, J.K., Hook, S.J., 1996. Mapping playa evaporite minerals and associated sediments in Death Valley, California, with multispectral thermal infrared images. J. Geophys. Res. 101, 643–660.
Dehouck, E., Mangold, N., LeMouélic, S., Ansan, V., Poulet, F., 2010. Ismenius Cavus, Mars: A deep paleolake with phyllosilicate deposits. Planet. Space Sci. 58, 941–946.
Ehlmann, B.L. et al., 2008a. Orbital identification of carbonate-bearing rocks on Mars. Science 322, 1828–1832.
Ehlmann, B.L., Mustard, J.F., Fassett, C.I., Schon, S.C., Head III, J.W., et al., 2008b. Clay minerals in delta deposits and organic preservation potential on Mars. Nat. Geosci. 355, 358.
Eugster, H.P., Hardie, L.A., 1978. Saline lakes. In: Lerman, A. (Ed.), Lakes-Chemistry, Geology, Physics. Springer-Verlag, New York, pp. 238–293.
Fairén, A.G. et al., 2010. Noachian and more recent phyllosilicates in impact craters on Mars. Publ. Natl. Acad. Sci., 12095–12100. doi:10.1073/pnas.1002889107.
Forsythe, R.D., Blackwelder, C.R., 1998. Closed drainage crater basins of the martian highlands: Constraints on the early martian hydrological cycle. J. Geophys. Res. 103, 31421–31431.
Gaffey, S.J., 1986. Spectral reflectance of carbonate minerals in the visible and near infrared (0.35–2.55 microns): Calcite, aragonite, dolomite. Am. Mineral. 71, 151–162.
Gaffey, S.J., 1987. Spectral reflectance of carbonate minerals in the visible and near infrared (0.35–2.55 μm): Anhydrous carbonate minerals. J. Geophys. Res. 82, 1429–1440.
Greeley, R., Guest, J.E., 1987. Geological Map of the Eastern Equatorial Region of Mars. US Geological Survey Map I-1802-B. United States Geological Survey.
Hartmann, W.K., Neukum, G., 2001. Cratering chronology and the evolution of Mars. Space Sci. Rev. 96, 165–194.
Ivanov, B.A., 2001. Mars/Moon cratering rate ratio estimates. Space Sci. Rev. 96, 87–104.
Kenkmann, T., Jahn, A., Scherler, D., Ivanov, B.A., 2005. Structure and formation of a central uplift: A case study at the Upheaval Dome impact crater, Utah. Geol. Soc. Am. Spec. Pap. 384, 85–115.
Malin, M.C. et al., 2007. Context camera investigation on board the Mars reconnaissance orbiter. J. Geophys. Res. 112, E05S04. doi:10.1029/2006JE002808.
Marzo, G.A., Davilia, A.F., Tornabene, L.L., Dohm, J.M., Gross, C., Kneissl, T., Bishop, J.L., Roush, T.L., McKay, C.P., 2010. Evidence for Hesperian impact-induced hydrothermalism on Mars. Icarus 208, 667–683. doi:10.1016/j.icarus.2010.03.013.
McEwen, A. et al., 2007. Mars reconnaissance orbiter's High Resolution Imaging Science Experiment (HiRISE). J. Geophys. Res. 112, E05S02. doi:10.1029/2005JE002605.
McGuire, P.C. et al., 2009. An improvement to the volcano-scan algorithm for atmospheric correction of CRISM and OMEGA spectral data. Planet. Space Sci. 57, 809–815.
Michael, G., Neukum, G., 2010. Planetary surface dating from crater size–frequency distribution measurements: Partial resurfacing events and statistical age uncertainty. Earth Planet. Sci. Lett. 294, 223–229.
Michalski, J.R., Niles, P.B., 2010. Deep crustal carbonate rocks exposed by meteor impacts on Mars. Nat. Geosci. doi:10.1038/NGEO971.
Milliken, R., Bish, D., 2010. Sources and sinks of clay minerals on Mars. Philos. Mag. 90, 2293–2308.
Murchie, S.M. et al., 2007. Compact reconnaissance imaging spectrometer for Mars (CRISM) on Mars reconnaissance orbiter (MRO). J. Geophys. Res. 112, E05S03. doi:10.1029/2006JE002682.
Murchie, S.M. et al., 2009. A synthesis of martian aqueous mineralogy after one Mars year of observations from the Mars reconnaissance orbiter. J. Geophys. Res. 114, E00D06. doi:10.1029/2009JE003342.
Mustard, J.F. et al., 2008. Hydrated silicate minerals on Mars observed by the CRISM instrument on MRO. Nature 454, 305–309.
Neukum, G., Jaumann, R., and the HRSC Team, 2004. The High Resolution Stereo Camera of Mars Express, in Mars Express: The Scientific Payload, ESA SP-1240. ESA Publ. Div. European Space Agency, Joordwijk, the Netherlands, pp. 17–35.
Orofino, V., Goldspeil, J., Carofalo, I., Blanco, A., Fonti, S., Marzo, G.A., 2009. Evaluation of carbonate abundance in putative martian paleolake basins. Icarus 200, 426–435. doi:10.1016/j.icarus.2008.11.020.
Palomba, E., Zinzi, A., Cloutis, E.A., D'Amore, M., Grassi, D., Maturilli, A., 2009. Evidence for Mg-rich carbonates on Mars from a 3.9 μm absorption feature. Icarus 203, 58–65. doi:10.1016/j.icarus.2009.04.013.
Parente, M., 2008. A New Approach to Denoising CRISM Images. Lunar Planet. Sci. Conf. 39. Lunar and Planetary Institute, Houston, Texas (abstract #2528).
Pelkey, S.M. et al., 2007. CRISM multispectral summary products: Parameterizing mineral diversity on Mars from reflectance. J. Geophys. Res. 112, E08S14. doi:10.1029/2006JE002831.
Roush, T., Marzo, G., Fonti, S., Orofino, V., Blanco, A., 2009. The search for evidence of aqueous activity in putative paleolake basins on Mars using CRISM spectral data. 2009 European Planet. Sci. Cong. (abstract EPSC2009-90).
Salvatore, M.R., Mustard, J.F., Wyatt, M.B., Murchie, S.L., 2010. Definitive evidence of Hesperian basalt in Acidalia and Chryse Planitiae. J. Geophys. Res. – Planets 115, E07005. doi:10.1029/2009JE003519.
Stockstill, K.R., Moersch, J.E., Ruff, S.W., Baldridge, A., Farmer, J., 2005. Thermal emission spectrometer hyperspectral analyses of proposed paleolake basins on Mars: No evidence for in-place carbonates. J. Geophys. Res. 110, E10004. doi:10.1029/2004JE002353.
Stockstill, K.R., Moersch, J.E., McSween, H.Y., Piatek, J., Christensen, P.R., 2007. TES and THEMIS study of proposed paleolake basins within the Aeolis quandrangle of Mars. J. Geophys. Res. 112, E01001. doi:10.1029/2005JE002517.
Tirsch, D., Jaumann, R., Pacifici, A., Poulet, F., 2011. Dark aeolian sediments in martian craters: Composition and sources. J. Geophys. Res. – Planets 116, E03002. doi:10.2029/2009JE003562.
Wray, J.J., Murchie, S.L., Squyres, S.W., Seelos, F.P., Tornabene, L.L., 2009. Diverse aqueous environments on ancient Mars revealed in the southern highlands. Geology 37, 1043–1046. doi:10.1130/G30331A.1.
Wray, J., Milliken, R., Dundas, C., Swayze, G., Andrews-Hanna, J., Baldridge, A., Chojnackiet, M., et al., 2011. Columbus crater and other possible groundwater-fed paleolakes of Terra Sirenum, Mars. J. Geophys. Res. – Planets 116, E01001. doi:10.2029/2010JE003694.